Antiviral Research 167 (2019) 1–5

Contents lists available at ScienceDirect

Antiviral Research

journal homepage: www.elsevier.com/locate/antiviral

Cell line-dependent activation and antiviral activity of T-1105, the non-fluorinated analogue of T-705 (favipiravir)

Johanna Huchting[a,b,*,1], Evelien Vanderlinden[a,1], Ria Van Berwaer[a], Chris Meier[b], Lieve Naesens[a,**]

[a] KU Leuven, Rega Institute for Medical Research, Herestraat 49, B-3000 Leuven, Belgium
[b] University of Hamburg, Faculty of Sciences, Department of Chemistry, Organic Chemistry, Martin-Luther-King-Platz 6, D-20146 Hamburg, Germany

ARTICLE INFO

Keywords:
Favipiravir
Antiviral
Cell line dependency
Activation
Nicotinamide mononucleotide analogue

ABSTRACT

The antiviral drug T-705 (favipiravir) and its non-fluorinated analogue T-1105 inhibit the polymerases of RNA viruses after being converted to their ribonucleoside triphosphate (RTP) metabolite. We here compared the activation efficiency of T-705 and T-1105 in four cell lines that are commonly used for their antiviral evaluation. In MDCK cells, the levels of T-705-RTP were markedly lower than those of T-1105-RTP, while the opposite was seen in A549, Vero and HEK293T cells. In the latter three cell lines, T-1105 activation was hindered by inefficient conversion of the ribonucleoside monophosphate to the ribonucleoside diphosphate *en route* to forming the active triphosphate. Accordingly, T-1105 had better anti-RNA virus activity in MDCK cells, while T-705 was more potent in the other three cell lines. Additionally, we identified a fourth metabolite, the NAD analogue of T-705/T-1105, and showed that it can be formed by nicotinamide mononucleotide adenylyltransferase.

1. Introduction

The broad antiviral drug T-705 (favipiravir; 6-fluoro-3-hydroxy-2-pyrazinecarboxamide) is known to function as a purine pseudobase, as evidenced by biochemical and cell culture studies (Furuta et al., 2005; Naesens et al., 2013; Jin et al., 2013; Sangawa et al., 2013). To exert its antiviral effect, T-705 requires conversion (Fig. 1A), first to its ribonucleoside 5′-monophosphate (T-705-RMP) by hypoxanthine guanine phosphoribosyltransferase (HGPRT) (Naesens et al., 2013), and next to the ribonucleoside 5′-diphosphate (T-705-RDP) and -triphosphate (T-705-RTP) metabolites (Smee et al., 2009; Sangawa et al., 2013; Bixler et al., 2018). At high concentrations, T-705-RTP shuts off RNA synthesis by influenza virus polymerase (Furuta et al., 2005; Sangawa et al., 2013; Jin et al., 2013). At lower concentrations, the drug acts as an RNA virus mutagen (Baranovich et al., 2013; Vanderlinden et al., 2016; Goldhill et al., 2018, 2019).

In a previous chemical investigation, we found that T-705 is chemically unstable when engaged in a nucleoside, impeding further synthetic explorations (Huchting et al., 2017). In contrast, the non-fluorinated analogue T-1105 ribonucleoside proved a useful precursor for the synthesis of T-1105-RMP, -RDP and -RTP and corresponding prodrugs (Huchting et al., 2018). Compared to T-705, T-1105 displayed stronger potency in influenza virus-infected Madin-Darby canine kidney (MDCK) cells; furthermore, T-1105-RTP proved 5-fold more potent than T-705-RTP when evaluated for inhibition of influenza virus polymerase (Huchting et al., 2018).

In the present study, we compared the metabolic profile of T-705 and T-1105. The RMP, RDP and RTP plus any other metabolites were quantified in four different cell lines. Striking cell line dependency in formation of T-1105-RTP was observed, with MDCK cells achieving the highest levels. The step from the RMP to RDP metabolite appeared to be a limiting bottleneck, especially in cells other than MDCK. This effect was less pronounced for T-705 and explained why, in A549 and Vero cells, T-705 had higher antiviral activity than T-1105, while the opposite was seen in MDCK cells. Also, we are the first to discover NAD-analogous metabolites of T-705 and T-1105, which we termed T-705- and T-1105-RAD. We propose that they are formed from T-705/T-1105-RMP by nicotinamide mononucleotide adenylyltransferase (NMNAT).

* Corresponding author. Present address: University of Hamburg, Faculty of Sciences, Department of Chemistry, Organic Chemistry, Martin-Luther-King-Platz 6, D-20146 Hamburg, Germany.
** Corresponding author. KU Leuven, Rega Insitute for Medical Research, Herestraat 49, B-3000 Leuven, Belgium.
E-mail addresses: johanna.huchting@chemie.uni-hamburg.de (J. Huchting), evelien.vanderlinden@kuleuven.be (E. Vanderlinden), chris.meier@chemie.uni-hamburg.de (C. Meier), lieve.naesens@kuleuven.be (L. Naesens).
[1] These Authors contributed equally.

https://doi.org/10.1016/j.antiviral.2019.04.002
Received 5 March 2019; Received in revised form 29 March 2019; Accepted 1 April 2019
Available online 02 April 2019

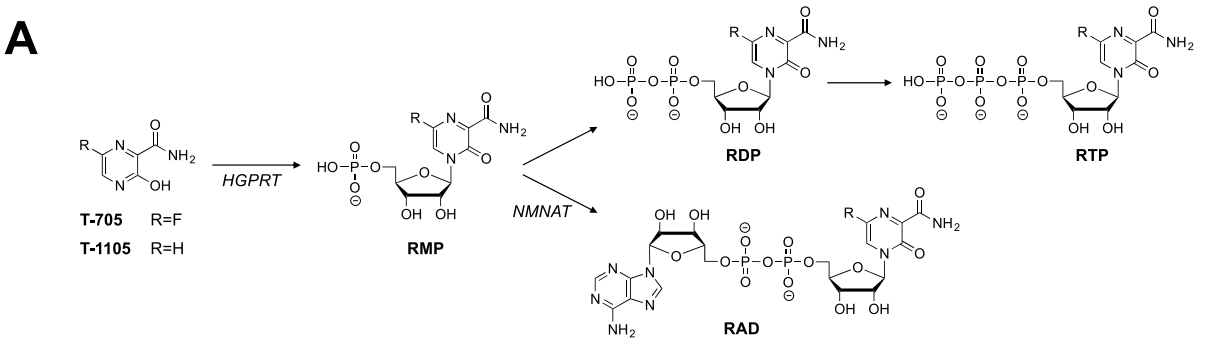

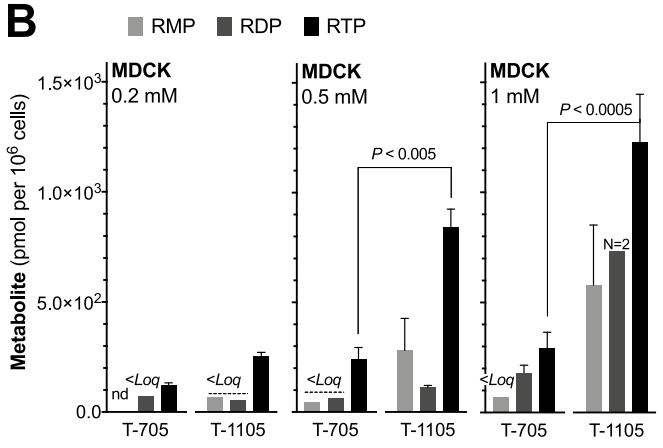

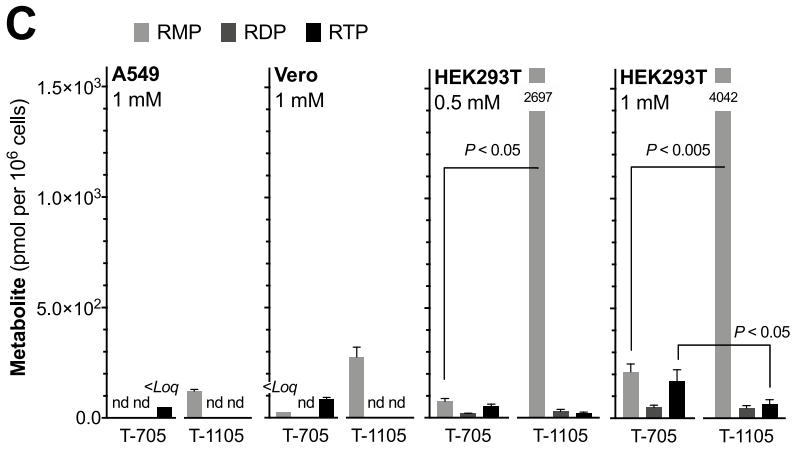

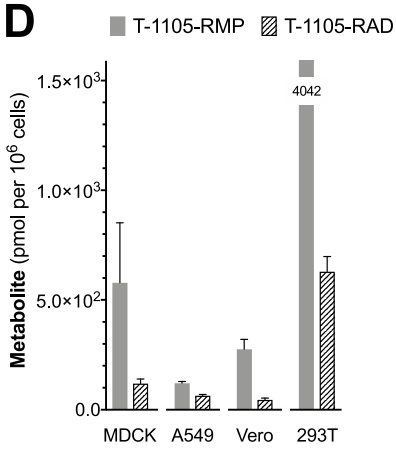

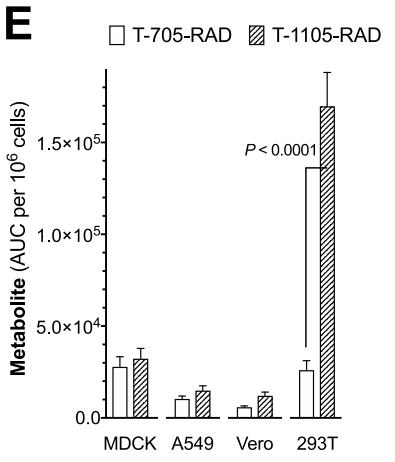

F

Antiviral assays		T-705	T-1105
Influenza A virus			
EC_{99} (μM)	MDCK	32 ± 3	6.0 ± 0.5
	A549	42 ± 11	146 ± 18
Parainfluenza-3 virus			
EC_{50} (μM)	MDCK	67 ± 18	17 ± 2
	Vero	8.9 ± 0.5	26 ± 4
Punta Toro virus			
EC_{50} (μM)	MDCK	50 ± 17	24 ± 5
	Vero	41 ± 2	>100
Replicon assay		**T-705**	**T-1105**
Influenza A virus			
EC_{50} (μM)	293T	70 ± 11	>100

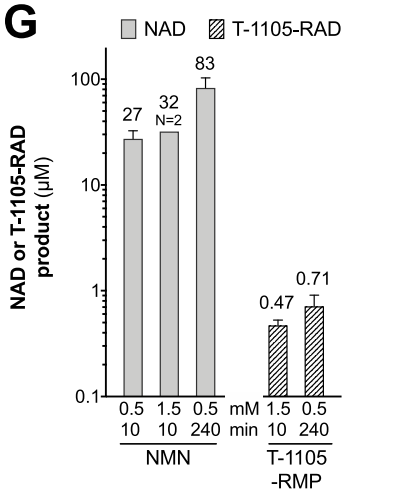

(caption on next page)

Fig. 1. Metabolism and antiviral potency of T-705 and T-1105 in MDCK, A549, Vero and HEK293T cells. (A) Metabolic activation pathway to convert T-705 and T-1105 into their active RTP metabolite (top). In a parallel reaction, the RMP is converted into the RAD metabolite (bottom). (B) Dose-dependent formation of the RMP, RDP and RTP metabolites in MDCK cells exposed to 0.2, 0.5 or 1 mM T-705 or T-1105. (C) Comparison of A549, Vero and HEK293T cells: RMP, RDP and RTP levels upon incubation with 0.5 or 1 mM T-705 or T-1105. nd: not detected; < Loq: above detection limit but below cutoff for reliable quantification. (D) Comparison of MDCK, A549, Vero and HEK293T cells: T-1105-RMP and -RAD levels upon incubation with 1 mM T-1105. (E) Comparison of T-705-RAD and T-1105-RAD levels in MDCK, A549, Vero and HEK293T cells upon incubation with 1 mM pseudobase. (F) Activity of T-705 and T-1105 in MDCK, A549 and Vero cells infected with influenza A virus, parainfluenza-3 virus and Punta Toro virus; and in the influenza virus replicon assay in HEK293T cells. EC_{99}: concentration affording 2-$\log_{10}$ reduction in virus titer; EC_{50}: concentration producing 50% inhibition of virus-induced cytopathic effect or influenza virus polymerase activity. (G) Enzymatic assay with hNMNAT3: conversion of NMN to NAD and T-1105-RMP to T-1105-RAD. All data are mean ± SEM of at least 3 biological replicates, unless specified differently in the figure.

2. Results and discussion

To study intracellular metabolic activation of T-705 and T-1105, we compared four cell lines which are commonly used for their antiviral evaluation. We and others have used MDCK cells for assessing the anti-influenza virus activity and mode of action of T-705 (Furuta et al., 2005; Smee et al., 2009; Baranovich et al., 2013; Vanderlinden et al., 2016). The compound was tested against several other RNA viruses using A549 or Vero cells (Oestereich et al., 2014; Delang et al., 2018; Furuta et al., 2017). The fourth cell line, HEK293T cells, is applied in the influenza virus replicon ('minigenome') assay to assess the inhibitory effect on viral RNA synthesis (Naesens et al., 2013; Goldhill et al., 2018). In our metabolism study, each of the four cell lines was kept in the same culture medium as that used for the antiviral experiments (see Supplementary Information for all details). By this we were able to analyze the relationship between antiviral activity and efficiency of metabolic activation.

Extracts from cells exposed to T-705 or T-1105 were submitted to anion-exchange HPLC. The metabolites were identified on the basis of their retention time (R_t) and UV spectrum, quantified from integrated peak areas (i.p.a.) using chemically synthesized T-705-RMP and T-1105-ribonucleotides for standardization, and values were normalized by number of analyzed cells. Depending on this number, reliable quantification was achieved from approx. 90 pmol per 10^6 cells (lower limit of quantification, i.e. 10xSD of i.p.a. from low concentrations divided by slope of standard curve and normalized by average cell count), and metabolites could still be detected at approx. 50 pmol per 10^6 cells (lower limit of detection). To agree with the conditions of the influenza replicon assay, HEK293T cells were used at 10-fold higher density and therefore, approx. 10-fold lower metabolite levels per 10^6 cells could be quantified.

In addition to the known T-705- and T-1105-ribonucleotides (i.e. RMP, RDP and RTP forms), we detected a fourth and previously unrecognized metabolite for both pseudobases. These novel forms had an R_t in between those of the RMP and RDP forms and close to that of NADH (for details regarding R_t see Supplementary Information, Metabolism experiment). Their UV-spectra contained a λ_{max} of 259 nm in addition to the λ_{max} of the corresponding pseudobase, i.e. 370 nm (T-705) or 350 nm (T-1105). Based on these characteristics, we hypothesized that these metabolites were NAD-analogous dinucleotides, wherein the nicotinamide base was replaced by the T-705/T-1105 pseudobase, and which we hence termed T-705- and T-1105-RAD (Fig. 1A). This was confirmed by identical analytical data from chemically synthesized T-1105-RAD (Chemical synthesis was achieved following the method described in Warnecke and Meier (2009), see Supplementary Information for all details).

In MDCK cells, metabolic activation of T-705 and T-1105 was dose-dependent and, when compared to the other three cell lines, relatively efficient (Fig. 1B). The RTP form achieved the highest levels among the four metabolites and T-1105 attained higher RTP levels than T-705 (Fig. 1B). The level of T-1105-RTP was 841 and 1228 pmol per 10^6 MDCK cells after 24 h incubation with 0.5 and 1 mM T-1105, respectively. About 4-fold lower RTP levels were observed for T-705; the differences in the levels of T-1105-RTP *versus* T-705-RTP were significant (*P*-value < 0.005; two-way ANOVA). Similar T-705-RTP concentrations were previously detected in MDCK cells by Smee et al. (2009). The superior RTP-formation of T-1105 in MDCK cells has not been observed before and at least partially explains why it is more potent than T-705 in inhibiting influenza virus replication in this cell line (see below).

The picture was entirely different in A549, Vero and HEK293T cells (Fig. 1C) since their levels of T-1105-RTP were far below those achieved in MDCK cells. This trend was less pronounced for T-705. At 1 mM, T-705 led to detectable RTP levels, which were significantly lower in A549 and Vero compared to MDCK cells (approx. 50 and 85 pmol per 10^6 A549 and Vero cells, respectively; *P*-value < 0.05 for comparison to the levels in MDCK cells; one-way ANOVA). T-1105-RTP was not detectable in A549 and Vero cells (i.e. < 50 pmol per 10^6 cells). Its level in HEK293T cells was 2.6-fold lower than that of T-705-RTP (i.e. 65 pmol and 171 pmol per 10^6 HEK293T cells, respectively).

In contrast to the RTP metabolites, RMP formation was generally more efficient for T-1105, since T-1105-RMP attained higher levels than T-705-RMP in all four cell lines (Fig. 1C). The difference was particularly striking in HEK293T cells: after 24 h incubation with 1 mM compound, T-705-RMP reached 212 pmol per 10^6 cells while T-1105-RMP reached a concentration as high as 4042 pmol per 10^6 cells. This may be related to our previous finding that, compared to T-705, T-1105 is a more efficient substrate for HGPRT-catalyzed phosphoribosylation (Naesens et al., 2013; Huchting et al., 2018). To compare compound activation efficiency in the different conditions, we calculated the RTP/RMP ratios. For T-705, the RTP/RMP ratio was > 1 in all conditions except for HEK293T cells, where it was 0.8 following 24 h treatment with 0.5 or 1 mM compound. This indicates that T-705-RMP is smoothly converted in all tested cell lines. For T-1105, an RTP/RMP ratio > 1 was seen in MDCK cells only (i.e. ratio of 4.2 and 2.8 under 0.5 and 1 mM T-1105, respectively). In the other three cell lines, the levels of T-1105-RTP were far below those of the RMP. In HEK293T cells exposed to 0.5 or 1 mM T-1105, the RTP/RMP ratio was 0.009 and 0.014, respectively. This means that in A549, Vero and HEK293T, but not MDCK cells, high T-1105-RMP levels do not translate into high T-1105-RTP levels. This could be due to restricted conversion of the RMP to RDP metabolite. As for conversion of the T-1105-RMP to RAD metabolite (Fig. 1A), this reaction appeared similarly efficient in all four cell lines and the T-1105-RAD/RMP ratio was in the range of 0.2–0.8 for all tested conditions (Fig. 1D). T-705-RAD was detected at similar levels compared to the non-fluorinated T-1105-RAD in MDCK, A549 and Vero cells (Fig. 1E). Only in HEK293T cells, T-705-RAD levels were significantly lower than T-1105-RAD (*P*-value < 0.0001 for 1 mM condition; two-way ANOVA), thus following the observed trend for the respective RMP levels. (As reported in Huchting et al. (2017), chemical synthesis of T-705 ribonucleotides is strongly impeded by chemical lability; thus, a synthetic T-705-RAD standard was not available, and AUC data were compared in Fig. 1E assuming similar extinction coefficients for T-705-RAD and T-1105-RAD at 370 and 350 nm, respectively).

Consequently, our metabolism data implicate that caution is warranted when the antiviral outcome of T-705 and T-1105 is being compared for different viruses in different cell lines. For T-705, cell line-dependent RTP formation was also observed by Bixler et al. (2018). Additionally, cell line-dependent potency of T-705 regarding

Chikungunya virus inhibition has been reported (Franco et al., 2018) and another recent study found that the drug inhibits Zika virus in Vero cells but not in different iPSC-derived neuronal cells (Lanko et al., 2017), indicating inadequate formation of T-705-RTP in some cell types. For this reason, we evaluated the two compounds against three different RNA viruses using MDCK, A549 and Vero cells (Fig. 1F). Since in our experiments the influenza virus did not give cytopathic effect in A549 cells, values yielding 2-log reduction in virus titers (EC_{99}) were compared here, while for parainfluenza and Punta Toro virus, values yielding 50%-reduction of cytopathic effect (EC_{50}) are given. In MDCK cells, T-1105 was more active than T-705, the fold difference in potency being 5 (influenza virus), 4 (parainfluenza virus) or 2 (Punta Toro virus). Compound ranking was reversed in A549 and Vero cells: T-705 was 3-fold more active than T-1105 in influenza virus-infected A549 cells and parainfluenza virus-infected Vero cells. In Vero cells infected with Punta Toro virus, T-705 was again moderately active while T-1105 was inactive (maximum tested concentration: 100 μM). Likewise, in the influenza virus replicon assay in HEK293T cells (Naesens et al., 2013), T-705 was active while T-1105 was not (Fig. 1F). In combination, these antiviral results nicely agree with our finding that T-1105-RTP formation is very efficient in MDCK cells but inadequate in A549, Vero and HEK293T cells. This cell line dependency is less pronounced for T-705.

In the final part of this study, we investigated the metabolic route and biological relevance of the T-705/T-1105-RAD metabolite which has not been identified before. This extra metabolite was formed in all four cell lines studied above (Fig. 1E) but not in MDCK-TG^{res} cells (Naesens et al., 2013) which are HGPRT-deficient and thus unable to phosphoribosylate T-705 and T-1105 (data not shown). Hence, formation of (at least) the RMP metabolite is required to generate the RAD metabolite (Fig. 1A). NAD-analogous metabolites have been reported for the carboxamide nucleobase-modified compounds tiazofurin, selenazofurin and benzamide riboside (Cooney et al., 1983; Gebeyehu et al., 1985; Gharehbaghi et al., 1994). The monophosphate forms of these nucleoside analogues are converted to the NAD metabolites by nicotinamide mononucleotide adenylyltransferase (NMNAT) which normally produces NAD from nicotinamide mononucleotide (NMN) and ATP (Cooney et al., 1983; Jaeger et al., 2002). Similarly, we found that hNMNAT3 converts T-1105-RMP to T-1105-RAD, though at an efficiency far below that of the natural NMN substrate (Fig. 1G; methodology in Supplementary Information). Reciprocally, even at 1 mM, T-1105-RMP did not inhibit the natural reaction with 0.3 mM NMN and 1 mM ATP.

The NAD analogues of tiazofurin, selenazofurin and benzamide riboside are known inhibitors of IMP dehydrogenase (IMPDH) (Cooney et al., 1983; Gebeyehu et al., 1985; Gharehbaghi et al., 1994; Jaeger et al., 2002). Suppression of this central enzyme in GMP biosynthesis leads to depletion of GTP and dGTP, explaining the use of IMPDH inhibitors for anticancer (Shah and Kharkar, 2018), immunosuppressive or antiviral therapy, as exemplified by ribavirin (Vanderlinden et al., 2016; Debing et al., 2014; Leyssen et al., 2005). Since the negative charges of T-705- and T-1105-RAD preclude their direct evaluation regarding any dose-dependent effects in cell-based experiments, we tested T-1105-RAD in an enzymatic assay with human IMPDH type 2 (see Supplementary Information). With a 50% inhibitory concentration of 26 μM (conditions: 100 μM NAD and 300 μM IMP), T-1105-RAD classified as a weak inhibitor. As expected for a structural analogue of NAD, its inhibitory potency was reduced at higher NAD concentrations. Thus, it may be assumed that the level of T-1105-RAD that is generated in cells exposed to T-1105, is too low to have relevance in terms of IMPDH inhibition or related antiviral outcome.

Our study revealed that compared to T-705, T-1105 is more cell line-dependent in terms of activation efficiency. In the four cell lines studied, T-1105 is more efficiently converted to the RMP than T-705, yet in A549, Vero and HEK293T cells, it is severely restricted at the subsequent steps to the RDP and RTP metabolites. The underlying reasons are currently unknown. Most plausibly, expression or activity of the activating enzymes may be dependent on the cell line or its proliferative status. To answer this, full knowledge of the activating enzymes is required. On the other hand, conversion of the RMP to the newly identified RAD metabolite did not show this drastic cell line dependency and hNMNAT3 was identified as a candidate enzyme performing this reaction. Our data contradict a strong inhibitory effect of T-1105-RAD on IMPDH. Further, no toxicity was observed in cells treated with T-705 or T-1105, which implies that RAD metabolites might not have harmful effects in these models. Still, since NAD is involved in many processes like cell metabolism, signaling and maintenance, these T-705/T-1105-RAD metabolites deserve to be further investigated.

Taken together, our data highlight the need to develop relevant, physiological models when aiming to evaluate and compare efficacy of antiviral candidates, which require activation by host enzymes, especially with regards to prioritizing compounds for clinical development. In terms of developing nucleobase or nucleoside analogues as broad-acting antivirals, our results further emphasize the potential represented by di- and triphosphate prodrugs to overcome (cell type-dependent) limitations.

Conflicts of interest

The authors have no competing interests to declare.

Acknowledgements

The work of J.H. was supported by a Postdoc-fellowship awarded by the German Academic Exchange Service (Deutscher Akademischer Austauschdienst, DAAD). The authors are grateful to Leentje Persoons and her team for excellent technical assistance.

Appendix A. Supplementary data

Supplementary data to this article can be found online at https://doi.org/10.1016/j.antiviral.2019.04.002.

Funding

This research did not receive any specific grant from funding agencies in the public, commercial, or not-for-profit sectors.

References

Baranovich, T., Wong, S.-S., Armstrong, J., Marjuki, H., Webby, R.J., Webster, R.G., Govorkova, E.A., 2013. T-705 (favipiravir) induces lethal mutagenesis in influenza A H1N1 viruses in vitro. J. Virol. 87, 3741–3751. https://doi.org/10.1128/JVI.02346-12.

Bixler, S.L., Bocan, T.M., Wells, J., Wetzel, K.S., Van Tongeren, S.A., Garza, N.L., Donnelly, G., Cazares, L.H., Soloveva, V., Welch, L., Epstein, C., Liang, L.F., Giesing, D., Lenk, R., Bavari, S., Warren, T.K., 2018. Intracellular conversion and in vivo dose response of favipiravir (T-705) in rodents infected with Ebola virus. Antivir. Res. 151, 50–54. https://doi.org/10.1016/j.antiviral.2017.12.020.

Cooney, D.A., Jayaram, H.N., Glazer, R.I., Kelley, J.A., Marquez, V.E., Gebeyehu, G., Van Cott, A.C., Zwelling, L.A., Johns, D.G., 1983. Studies on the mechanism of action of tiazofurin metabolism to an analog of NAD with potent IMP dehydrogenase-inhibitory activity. Adv. Enzym. Regul. 21, 271–303. https://doi.org/10.1016/0065-2571(83)90019-5.

Debing, Y., Emerson, S.U., Wang, Y., Pan, Q., Balzarini, J., Dallmeier, K., Neyts, J., 2014. Ribavirin inhibits in vitro hepatitis E virus replication through depletion of cellular GTP pools and is moderately synergistic with alpha interferon. Antimicrob. Agents Chemother. 58, 267–273. https://doi.org/10.1128/AAC.01795-13.

Delang, L., Abdelnabi, R., Neyts, J., 2018. Favipiravir as a potential countermeasure against neglected and emerging RNA viruses. Antivir. Res. 153, 85–94. https://doi.org/10.1016/j.antiviral.2018.03.003.

Franco, E.J., Rodriquez, J.L., Pomeroy, J.J., Hanrahan, K.C., Brown, A.N., 2018. The effectiveness of antiviral agents with broad-spectrum activity against chikungunya virus varies between host cell lines. Antiviral Chem. Chemother. 26, 1–7. https://doi.org/10.1177/2040206618807580.

Furuta, Y., Takahashi, K., Kuno-Maekawa, M., Sangawa, H., Uehara, S., Kozaki, K., Nomura, N., Egawa, H., Shiraki, K., 2005. Mechanism of action of T-705 against

influenza virus. Antimicrob. Agents Chemother. 49, 981–986. https://doi.org/10.1128/AAC.49.3.981-986.2005.
Furuta, Y., Komeno, T., Nakamura, T., 2017. Favipiravir (T-705), a broad spectrum inhibitor of viral RNA polymerase. Proc. Jpn. Acad. Ser. B Phys. Biol. Sci. 93, 449–463. https://doi.org/10.2183/pjab.93.027.
Gebeyehu, G., Marquez, V.E., Van Cott, A., Cooney, D.A., Kelley, J.A., Jayaram, H.N., Ahluwalia, G.S., Dion, R.L., Wilson, Y.A., Johns, D.G., 1985. Ribavirin, tiazofurin, and selenazofurin: mononucleotides and nicotinamide adenine dinucleotide analogues. Synthesis, structure, and interactions with IMP dehydrogenase. J. Med. Chem. 28, 99–105. https://doi.org/10.1021/jm00379a018.
Gharehbaghi, K., Paull, K.D., Kelley, J.A., Barchi, J.J., Marquez, V.E., Cooney, D.A., Monks, A., Scudiero, D., Krohn, K., Jayaram, H.N., 1994. Cytotoxicity and characterization of an active metabolite of benzamide riboside, a novel inhibitor of IMP dehydrogenase. Int. J. Cancer 56, 892–899. https://doi.org/10.1002/ijc.2910560623.
Goldhill, D.H., Te Velthuis, A.J.W., Fletcher, R.A., Langat, P., Zambon, M., Lackenby, A., Barclay, W.S., 2018. The mechanism of resistance to favipiravir in influenza. Proc. Natl. Acad. Sci. U.S.A. 115, 11613–11618. https://doi.org/10.1073/pnas.1811345115.
Goldhill, D., Langat, P., Xie, H., Galiano, M., Miah, S., Kellam, P., Zambon, M., Lackenby, A., Barclay, W.S., 2019. Determining the mutation bias of favipiravir in influenza using next-generation sequencing. J. Virol. 93, e01217–e01218. https://doi.org/10.1128/JVI.01217-18 Preprint posted on bioRxiv July 23, 2018 (bioRxiv:10.1101/375378).
Huchting, J., Winkler, M., Nasser, H., Meier, C., 2017. Synthesis of T-705-ribonucleoside and T-705-ribonucleotide and studies of chemical stability. ChemMedChem 12, 652–659. https://doi.org/10.1002/cmdc.201700116.
Huchting, J., Vanderlinden, E., Winkler, M., Nasser, H., Naesens, L., Meier, C., 2018. Prodrugs of the phosphoribosylated forms of hydroxypyrazinecarboxamide pseudobase T-705 and its de-fluoro analogue T-1105 as potent influenza virus inhibitors. J. Med. Chem. 61, 6193–6210. https://doi.org/10.1021/acs.jmedchem.8b00617.
Jaeger, W., Salamon, A., Szekeres, T., 2002. Metabolism of the novel IMP dehydrogenase inhibitor benzamide riboside. Curr. Med. Chem. 9, 781–786.
Jin, Z., Smith, L.K., Rajwanshi, V.K., Kim, B., Deval, J., 2013. The ambiguous base-pairing and high substrate efficiency of T-705 (Favipiravir) ribofuranosyl 5′-triphosphate towards influenza A virus polymerase. PLoS One 8, e68347. https://doi.org/10.1371/journal.pone.0068347.
Lanko, K., Eggermont, K., Patel, A., Kaptein, S., Delang, L., Verfaillie, C.M., Neyts, J., 2017. Replication of the Zika virus in different iPSC-derived neuronal cells and implications to assess efficacy of antivirals. Antivir. Res. 145, 82–86. https://doi.org/10.1016/j.antiviral.2017.07.010.
Leyssen, P., Balzarini, J., De Clercq, E., Neyts, J., 2005. The predominant mechanism by which ribavirin exerts its antiviral activity in vitro against flaviviruses and paramyxoviruses is mediated by inhibition of IMP dehydrogenase. J. Virol. 79, 1943–1947. https://doi.org/10.1128/JVI.79.3.1943-1947.2005.
Naesens, L., Guddat, L.W., Keough, D.T., van Kuilenburg, A.B.P., Meijer, J., Vande Voorde, J., Balzarini, J., 2013. Role of human hypoxanthine guanine phosphoribosyltransferase in activation of the antiviral agent T-705 (favipiravir). Mol. Pharmacol. 84, 615–629. https://doi.org/10.1124/mol.113.087247.
Oestereich, L., Ludtke, A., Wurr, S., Rieger, T., Munoz-Fontela, C., Gunther, S., 2014. Successful treatment of advanced Ebola virus infection with T-705 (favipiravir) in a small animal model. Antivir. Res. 105, 17–21. https://doi.org/10.1016/j.antiviral.2014.02.014.
Sangawa, H., Komeno, T., Nishikawa, H., Yoshida, A., Takahashi, K., Nomura, N., Furuta, Y., 2013. Mechanism of action of T- 705 ribosyl triphosphate against influenza virus RNA polymerase. Antimicrob. Agents Chemother. 57, 5202–5208. https://doi.org/10.1128/AAC.00649-13.
Shah, C.P., Kharkar, P.S., 2018. Discovery of novel human inosine 5'-monophosphate dehydrogenase 2 (hIMPDH2) inhibitors as potential anticancer agents. Eur. J. Med. Chem. 158, 286–301. https://doi.org/10.1016/j.ejmech.2018.09.016.
Smee, D.F., Hurst, B.L., Egawa, H., Takahashi, K., Kadota, T., Furuta, Y., 2009. Intracellular metabolism of favipiravir (T-705) in uninfected and influenza A (H5N1) virus-infected cells. J. Antimicrob. Chemother. 64, 741–746. https://doi.org/10.1093/jac/dkp274.
Vanderlinden, E., Vrancken, B., Van Houdt, J., Rajwanshi, V.K., Gillemot, S., Andrei, G., Lemey, P., Naesens, L., 2016. Distinct effects of T-705 (favipiravir) and ribavirin on influenza virus replication and viral RNA synthesis. Antimicrob. Agents Chemother. 60, 6679–6691. https://doi.org/10.1128/AAC.01156-16.
Warnecke, S., Meier, C., 2009. Synthesis of nucleoside Di- and triphosphates and dinucleoside polyphosphates with *cyclo*Sal-nucleotides. J. Org. Chem. 74, 3024–3030. https://doi.org/10.1021/jo802348h.